

A Fractal-Fractional Model for the MHD Flow of Casson Fluid in a Channel

Nadeem Ahmad Sheikh^{1,2}, Dennis Ling Chuan Ching¹, Thabet Abdeljawad^{3,4,5}, Ilyas Khan^{6,*},
Muhammad Jamil^{7,8} and Kottakkaran Sooppy Nisar⁹

¹Fundamental and Applied Science Department, Universiti Teknologi PETRONAS, Perak, 32610, Malaysia

²Department of Mathematics, City University of Science and Information Technology, Peshawar, 25000, Pakistan

³Department of Mathematics and General Sciences, Prince Sultan University, 11586, Riyadh, Saudi Arabia

⁴Department of Medical Research, China Medical University, 40402, Taichung, Taiwan

⁵Department of Computer Science and Information Engineering, Asia University, Taichung, Taiwan

⁶Faculty of Mathematics and Statistics, Ton Duc Thang University, Ho Chi Minh City, 72915, Vietnam

⁷Department of Geosciences, Universiti Teknologi PETRONAS, Perak, 32610, Malaysia

⁸Department of Earth Sciences, COMSATS University Islamabad, Abbottabad Campus, Abbottabad, 22010, Pakistan

⁹Department of Mathematics, College of Arts and Sciences, Prince Sattam bin Abdulaziz University, Wadi Aldawaser, 11991, Saudi Arabia

*Corresponding Author: Ilyas Khan. Email: ilyaskhan@tdtu.edu.vn

Received: 08 June 2020; Accepted: 26 July 2020

Abstract: An emerging definition of the fractal-fractional operator has been used in this study for the modeling of Casson fluid flow. The magnetohydrodynamics flow of Casson fluid has cogent in a channel where the motion of the upper plate generates the flow while the lower plate is at a static position. The proposed model is non-dimensionalized using the Pi-Buckingham theorem to reduce the complexity in solving the model and computation time. The non-dimensional fractal-fractional model with the power-law kernel has been solved through the Laplace transform technique. The Mathcad software has been used for illustration of the influence of various parameters, i.e., Hartman number, fractal, fractional, and Casson fluid parameters on the velocity of fluid flow. Through graphs and tables, the results have been implemented and it is shown that the boundary conditions are fully satisfied. The results reveal that the flow velocity is decreasing with the increasing values of the Hartman number and is increasing with the increasing values of the Casson fluid parameter. The findings of the fractal-fractional model have elucidated that the memory effect of the flow model has higher quality than the simple fractional and classical models. Furthermore, to show the validity of the obtained closed-form solutions, special cases have been obtained which are in agreement with the already published solutions.

Keywords: Fractal-fractional derivative; Casson fluid; MHD flow; exact solutions

Nomenclature

μ	dynamic viscosity
ρ	the fluid density
e_{ij}	the $(i, j)^{th}$ component of deformation rate



This work is licensed under a Creative Commons Attribution 4.0 International License, which permits unrestricted use, distribution, and reproduction in any medium, provided the original work is properly cited.

p_y	the yield stress of the non-Newtonian fluid
$\pi = e_{ij}e_{ij}$	the product of the component of deformation rate itself
π_c	the critical value of this product based on the non-Newtonian model
μ_γ	the plastic dynamic viscosity
β	the material parameter of Casson fluid
u	the fluid velocity in the x -direction

1 Introduction

The applications of non-Newtonian fluids are quite remarkable and play an important role in the flow modeling in industry and engineering sectors [1–4]. The magnetohydrodynamic (MHD) flows of these fluids are widely used in the field of MHD generators, magnetic drug targeting (MDT), MRI, and controlled flows, etc. with increased interest by many researchers [3,5,6]. Non-Newtonian fluids exhibit a complex structure that essentially requires some robust mathematical modeling for explanation and depiction. The non-Newtonian fluids flow behaves inversely with the influence of porosity and magnetohydrodynamics [2]. To solve the model for the MHD flow of micropolar fluid, the Laplace transformation was applied by Ali et al. [7]. MHD flow has been studied for the oscillating plates which include the effects of porous media under heat transfer and radiation [2,5]. The convective flow of non-Newtonian fluid over an oscillating plate in porous media was studied by Krishna et al. [8]. They have shown the relationship between the pressure gradient and flow velocity. This pressure gradient study has also discussed the relationship with the magnetohydrodynamics and the effects of different materials on the velocity using the Lattice Boltzmann method. The unsteady flow of Casson fluid for the oscillating plate to show the velocity relation in the porous media was studied by Khan et al. [9], who also discussed the velocity and shear stress by obtaining closed-form solutions. Ullah et al. [10] studied the flow of Casson fluid with slip on the stretching sheet.

Fractional derivatives are quite applicable for efficiently discussing the complex real-world problem for the flow of various types of fluids [11]. Several numerical simulations have studied water pollution with different applications through Caputo Fabrizio (CF) fractional derivatives [12]. These CF fractional derivatives have also been used in heat transfer analysis to get closed-form solutions for unsteady fluid flow over an oscillating plate where the fractional parameter is directly proportional to temperature. At the same time, it is inversely related to the velocity of the fluid. Fractional fluids have higher velocity values, which positively influence fluid flow [13]. These tenuous effects of the fluid flow could be efficiently resolved with the help of fractional derivatives [11]. The CF fractional derivatives and Atangana–Baleanu (AB) are very useful to identify and calculate the velocity values [14]. Fractional partial differential equations had also solved for closed-form solutions by using finite Hankel and Laplace transformation techniques. The numerical analysis of the fractional derivatives highlights a more significant effect on the velocity as compared to ordinary derivatives [15]. The fractional model could also apply to Casson fluid along with the energy equations. The Caputo fractional model and the Laplace transformation have also been used to get the solutions with Wright function by Ali et al. [16]. AB fractional derivatives and CF fractional derivatives could be used for the demonstration of the heat and mass transfer analysis of free convection flow of Casson fluid. For these types of flows, solutions and results were obtained through the Laplace transformation technique by Sheikh et al. [17]. Free convection generalized (Caputo–Fabrizio time-fractional derivatives) flow of Jeffrey fluid was analyzed via the Laplace transformation technique by Saqib et al. [18]. They had obtained the exact solutions for velocity and temperature. The results emphasize that fractional flows are relatively swifter than classical flows. Saqib et al. [11] discussed the Atangana–Baleanu (AB) derivatives model for Casson fluid in a microchannel. They have concluded that the fractional parameter considerably influences the viscosity

and buoyancy forces. The numerical analysis of nanofluids through a porous media in a vertical channel by applying AB fractional derivative for convection free flow was discussed by Saqib et al. [19]. The flow of Casson fluid was considered by Sheikh et al. [20]. They studied the Caputo fractional derivative and the flow had modeled using the generalized Fourier and Fick laws.

Carpinteri et al. [21] discussed the fractal-fractional calculus in continuum mechanics. The fractal-fractional model for the convective flow in the rotating cavity was considered by Abro et al. [22]. They used the Caputo fractional derivative, CF derivatives, and AB derivatives for their analysis. Fractal-fractional derivatives for Couette flow by Laplace transformation were applied for viscous fluid flow between two plates considering a constant value of velocity [23]. In many real-life phenomena, mathematical modeling with and without fractional calculus is quite applicable especially in engineering and sciences, for instance, [24–35] mathematical biology and infectious diseases [36], market economics [37], and biomedical research [38,39].

Keeping in mind the above literature survey, in this paper we have considered electrically conducted flow of Casson fluid in a channel. The fractal-fractional model has been created for the subject flow using the concept of fractional calculus. The exact solutions have been obtained using the Laplace transform technique.

2 Mathematical Modelling

We have considered the motion of Casson fluid in a vertical channel. The flow is assumed in the direction of the x -axis while the y -axis is taken perpendicular to the plates. The fluid and the plates are at rest when $t \leq 0$. At $t = 0^+$, the plate at $y = d$ begins to move in its plane with velocity U as shown in Fig. 1.

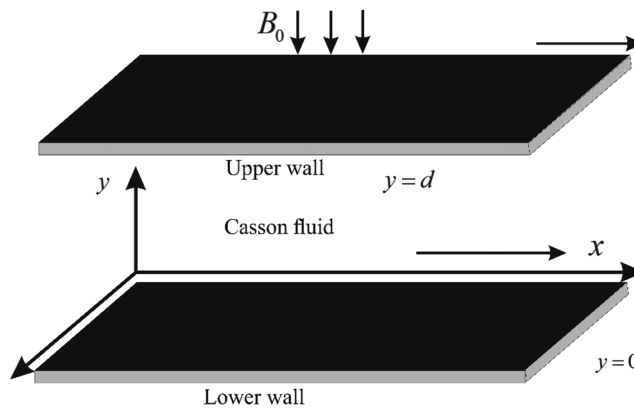


Figure 1: Geometry of the flow

We suppose that the rheological equation for an incompressible Casson fluid is [15,40]:

$$\tau_{ij} = \begin{cases} 2\left(\mu_\gamma + \frac{p_\gamma}{\sqrt{2\pi}}\right) e_{ij}, & \pi > \pi_c, \\ 2\left(\mu_\gamma + \frac{p_\gamma}{\sqrt{2\pi_c}}\right) e_{ij}, & \pi_c < \pi. \end{cases} \quad (1)$$

The flow of Casson fluid is governed by the following partial differential equations [41,42]:

$$\rho \frac{\partial u(y, t)}{\partial t} = \mu \left(1 + \frac{1}{\beta} \right) \frac{\partial^2 u(y, t)}{\partial y^2} - \sigma B_0^2 u(y, t), \quad (2)$$

where the initial and boundary conditions are:

$$u(y, 0) = 0, u(0, t) = 0, u(d, t) = U. \quad (3)$$

Introducing the following dimensionless variables [23]

$$v = \frac{u}{U}, \xi = \frac{U}{\nu} y, \tau = \frac{U^2}{\nu} t, \text{ into Eq. (2) and Eq. (3) we get:}$$

$$\frac{\partial v(\xi, \tau)}{\partial \tau} = \beta_0 \frac{\partial^2 v(\xi, \tau)}{\partial \xi^2} - Mv(\xi, \tau), \quad (4)$$

with initial and boundary conditions in the dimensionless form:

$$v(\xi, 0) = 0, v(0, \tau) = 0, v(1, \tau) = 1, \quad (5)$$

where $M = \frac{\sigma B_0^2 \nu}{\mu U^2}$ is the Hartman number and $\beta_0 = 1 + \frac{1}{\beta}$.

2.1 Fractal-Fractional Model

The fractal-fractional model for the mentioned flow problem, in the generalized form is:

$${}^C \partial_{\tau}^{\alpha} v(\xi, \tau) = \delta \tau^{\delta-1} \left(\beta_0 \frac{\partial^2 v(\xi, \tau)}{\partial \xi^2} - Mv(\xi, \tau) \right) - \frac{v(\xi, 0) \tau^{-\alpha}}{\Gamma(1-\alpha)}, \quad (6)$$

If we assume that $v(\kappa)$ is continuous in open interval, if $v(\kappa)$ is fractal differentiable on (a, b) with order δ , then the fractal fractional derivative of $v(\kappa)$ with order α in Riemann–Liouville sense with power law is presented as [43]

$${}^{FFP} \partial_{\kappa}^{\alpha, \delta} v(\kappa) = \frac{1}{\Gamma(1-\alpha)} \frac{d}{d\kappa^{\delta}} \int_a^{\kappa} v(t) (\kappa - t)^{-\alpha} dt, \quad (7)$$

where

$$\frac{dv(t)}{dt^{\delta}} = \lim_{\kappa \rightarrow t} \frac{v(\kappa) - v(t)}{\kappa^{\delta} - t^{\delta}}. \quad (8)$$

2.2 Velocity Profile

Applying the Laplace transform to Eq. (5) using Eq. (6) we arrived at

$$s^{\alpha} \bar{v}(\xi, s) - v(\xi, 0) = \delta \Gamma(\delta) s^{-\delta} \left(\beta_0 \frac{\partial^2 \bar{v}(\xi, s)}{\partial \xi^2} - M \bar{v}(\xi, s) \right), \quad (9)$$

in a suitable form Eq. (9) can be written as

$$\frac{\partial^2 \bar{v}(\xi, s)}{\partial \xi^2} = \frac{1}{\delta \Gamma(\delta) \beta_0} (s^{\alpha} + \delta \Gamma(\delta) M) \bar{v}(\xi, s), \quad (10)$$

solving Eq. (10), using Eq. (5) we have the following solution:

$$\bar{v}(\xi, s) = \frac{1}{s} \left[\frac{e^{-\xi \sqrt{a(s^{\alpha+\delta} + \delta\Gamma(\delta)M)}}}{e^{-\sqrt{a(s^{\alpha+\delta} + \delta\Gamma(\delta)M)}} - e^{\sqrt{a(s^{\alpha+\delta} + \delta\Gamma(\delta)M)}}} - \frac{e^{\xi \sqrt{a(s^{\alpha+\delta} + \delta\Gamma(\delta)M)}}}{e^{-\sqrt{a(s^{\alpha+\delta} + \delta\Gamma(\delta)M)}} - e^{\sqrt{a(s^{\alpha+\delta} + \delta\Gamma(\delta)M)}}} \right], \tag{11}$$

where $a = \frac{1}{\delta\Gamma(\delta)\beta_0}$.

In more suitable form Eq. (11) can be written as:

$$\bar{v}(\xi, s) = \frac{1}{s} \sum_{n=1}^{\infty} \left[\sum_{\chi_1}^{\infty} \frac{(2n+1-\xi)^{\chi_1}}{\chi_1!} \left(\sqrt{a(s^{\alpha+\delta} + \delta\Gamma(\delta)M)} \right)^{\chi_1} - \sum_{\chi_2}^{\infty} \frac{(-(2n+1-\xi))^{\chi_2}}{\chi_2!} \left(\sqrt{a(s^{\alpha+\delta} + \delta\Gamma(\delta)M)} \right)^{\chi_2} \right], \tag{12}$$

inverting the Laplace transformation of Eq. (12) [23] we have:

$$v(\xi, \tau) = \sum_{n=1}^{\infty} \left[\sum_{\chi_1}^{\infty} \sum_{\lambda_1}^{\infty} \left\{ \frac{(-2n-1+\xi)^{\chi_1} (\sqrt{a})^{\chi_1} (\delta\Gamma(\delta)M)^{\lambda_1}}{\chi_1! \lambda_1!} \frac{\tau^{\lambda_1 - \frac{(\alpha+\delta)\chi_1}{2}}}{\Gamma\left(1 + \lambda_1 - \frac{(\alpha+\delta)\chi_1}{2}\right)} \frac{\Gamma\left(\lambda_1 + \frac{\chi_1}{2}\right)}{\Gamma\left(\frac{\chi_1}{2}\right)} \right\} - \sum_{\chi_2}^{\infty} \sum_{\lambda_2}^{\infty} \left\{ \frac{(2n+1-\xi)^{\chi_2} (\sqrt{a})^{\chi_2} (\delta\Gamma(\delta)M)^{\lambda_2}}{\chi_2! \lambda_2!} \frac{\tau^{\lambda_2 - \frac{(\alpha+\delta)\chi_2}{2}}}{\Gamma\left(1 + \lambda_2 - \frac{(\alpha+\delta)\chi_2}{2}\right)} \frac{\Gamma\left(\lambda_2 + \frac{\chi_2}{2}\right)}{\Gamma\left(\frac{\chi_2}{2}\right)} \right\} \right] \tag{13}$$

2.3 Limiting Cases

Validating results, the present solutions have reduced to the already published results in the literature, and the solutions for some other well-known flows have been obtained.

2.3.1 Case 1 (Newtonian Fluid)

For $\beta \rightarrow \infty$ the obtained solution is reduced to the following form:

$$v(\xi, \tau) = \sum_{n=1}^{\infty} \left[\sum_{\chi_1}^{\infty} \sum_{\lambda_1}^{\infty} \left\{ \frac{(-2n-1+\xi)^{\chi_1} \left(\sqrt{\frac{1}{\delta\Gamma(\delta)}} \right)^{\chi_1} (\delta\Gamma(\delta)M)^{\lambda_1}}{\chi_1! \lambda_1!} \frac{\tau^{\lambda_1 - \frac{(\alpha+\delta)\chi_1}{2}}}{\Gamma\left(1 + \lambda_1 - \frac{(\alpha+\delta)\chi_1}{2}\right)} \frac{\Gamma\left(\lambda_1 + \frac{\chi_1}{2}\right)}{\Gamma\left(\frac{\chi_1}{2}\right)} \right\} - \sum_{\chi_2}^{\infty} \sum_{\lambda_2}^{\infty} \left\{ \frac{(2n+1-\xi)^{\chi_2} \left(\sqrt{\frac{1}{\delta\Gamma(\delta)}} \right)^{\chi_2} (\delta\Gamma(\delta)M)^{\lambda_2}}{\chi_2! \lambda_2!} \frac{\tau^{\lambda_2 - \frac{(\alpha+\delta)\chi_2}{2}}}{\Gamma\left(1 + \lambda_2 - \frac{(\alpha+\delta)\chi_2}{2}\right)} \frac{\Gamma\left(\lambda_2 + \frac{\chi_2}{2}\right)}{\Gamma\left(\frac{\chi_2}{2}\right)} \right\} \right], \tag{14}$$

which is identical to the solution calculated by [23].

2.3.2 Case 2 (Solution for fractional model)

For $\delta = 1$ the obtained solution is reduced to the corresponding fractional model:

$$v(\xi, \tau) = \sum_{n=1}^{\infty} \left[\sum_{\chi_1}^{\infty} \sum_{\lambda_1}^{\infty} \left\{ \frac{(-2n-1+\xi)^{\chi_1} (\sqrt{a})^{\chi_1} (M)^{\lambda_1}}{\chi_1! \lambda_1!} \frac{\tau^{\lambda_1 - \frac{(1+\alpha)\chi_1}{2}}}{\Gamma\left(1+\lambda_1 - \frac{(1+\alpha)\chi_1}{2}\right)} \frac{\Gamma\left(\lambda_1 + \frac{\chi_1}{2}\right)}{\Gamma\left(\frac{\chi_1}{2}\right)} \right\} - \sum_{\chi_2}^{\infty} \sum_{\lambda_2}^{\infty} \left\{ \frac{(2n+1-\xi)^{\chi_2} (\sqrt{a})^{\chi_2} (M)^{\lambda_2}}{\chi_2! \lambda_2!} \frac{\tau^{\lambda_2 - \frac{(1+\alpha)\chi_2}{2}}}{\Gamma\left(1+\lambda_2 - \frac{(1+\alpha)\chi_2}{2}\right)} \frac{\Gamma\left(\lambda_2 + \frac{\chi_2}{2}\right)}{\Gamma\left(\frac{\chi_2}{2}\right)} \right\} \right]. \tag{15}$$

2.3.3 Case 3 (Solution of integer order model)

For $\alpha = \delta = 1$ the obtained solution is reduced to the corresponding classical model:

$$v(\xi, \tau) = \sum_{n=1}^{\infty} \left[\sum_{\chi_1}^{\infty} \sum_{\lambda_1}^{\infty} \left\{ \frac{(-2n-1+\xi)^{\chi_1} (\sqrt{a})^{\chi_1} (M)^{\lambda_1}}{\chi_1! \lambda_1!} \frac{\tau^{\lambda_1 - \chi_1}}{\Gamma(1+\lambda_1 - \chi_1)} \frac{\Gamma\left(\lambda_1 + \frac{\chi_1}{2}\right)}{\Gamma\left(\frac{\chi_1}{2}\right)} \right\} - \sum_{\chi_2}^{\infty} \sum_{\lambda_2}^{\infty} \left\{ \frac{(2n+1-\xi)^{\chi_2} (\sqrt{a})^{\chi_2} (M)^{\lambda_2}}{\chi_2! \lambda_2!} \frac{\tau^{\lambda_2 - \chi_1}}{\Gamma(1+\lambda_2 - \chi_1)} \frac{\Gamma\left(\lambda_2 + \frac{\chi_2}{2}\right)}{\Gamma\left(\frac{\chi_2}{2}\right)} \right\} \right]. \tag{16}$$

3 Results and Discussion

In the present study, we have considered the fractal-fractional model of the MHD flow of Casson fluid in a channel. The flow has been induced due to the constant velocity of the upper plate. To better understand the flow behavior, graphs have been plotted for velocity profile, and the results shown in tables.

The influence of the Hartman number is shown in Fig. 2. The velocity of the Casson fluid is decreasing with the increasing values of the Hartman number. Lorentz’s forces, which are opposing forces to the flow, are more potent for the rising values of the Hartman number. This behavior is also shown in Tab. 1, which clearly shows that the obtained solutions are satisfying the imposed boundary conditions.

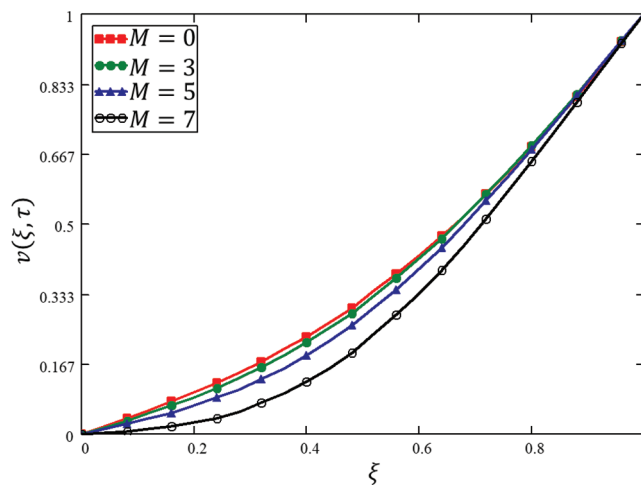


Figure 2: Variations in velocity profile against ξ for different values of M

Table 1: Variations in velocity profile against ξ for different values of M

ξ	$v(\xi, \tau)$ at $M = 0$	$v(\xi, \tau)$ at $M = 3$	$v(\xi, \tau)$ at $M = 5$	$v(\xi, \tau)$ at $M = 7$
0	0	0	0	0
0.04	0.019	0.016	0.012	$2.923e^{-3}$
0.08	0.038	0.033	0.024	$6.478e^{-3}$
0.12	0.057	0.05	0.037	0.011
0.16	0.078	0.068	0.051	0.018
0.2	0.099	0.088	0.068	0.027
0.24	0.122	0.11	0.086	0.039
0.28	0.147	0.133	0.107	0.054
0.32	0.173	0.159	0.131	0.074
0.36	0.202	0.187	0.158	0.097
0.4	0.232	0.218	0.188	0.125
0.44	0.265	0.252	0.222	0.158
0.48	0.301	0.289	0.259	0.195
0.52	0.339	0.329	0.3	0.237
0.56	0.38	0.372	0.345	0.284
0.6	0.424	0.418	0.393	0.336
0.64	0.471	0.466	0.444	0.391
0.68	0.52	0.518	0.499	0.451
0.72	0.572	0.572	0.556	0.514
0.76	0.627	0.629	0.616	0.58
0.8	0.684	0.688	0.678	0.649
0.84	0.743	0.748	0.742	0.719
0.88	0.805	0.81	0.806	0.79
0.92	0.868	0.873	0.871	0.861
0.96	0.933	0.937	0.936	0.931
1	1	1	1	1

The effect of the fractional parameter is shown in Fig. 3 and presented in Tab. 2. Variations in velocity are shown for different values of α , and despite the increasing or decreasing behavior of the velocity, this figure shows that we can draw many graphs for the velocity while keeping the physical parameters constant. This effect is known as a memory effect, which can be described by α .

The graph is plotted for δ in Fig. 4 and presented in Tab. 3. Despite the increasing or decreasing behavior of the velocity, this figure shows that we can draw many graphs for the velocity while keeping the physical parameters constant. The important fact is that both the fractional and fractal parameters are describing the memory, and together these can describe the memory better than the fractional and classical models.

To show the effect of the Casson fluid parameter β , Fig. 5 has been plotted. It has been depicted from this figure that velocity increases with the increasing values of β . Physically, the increasing values of β reduces the thickness of the boundary layer. We can say that for a huge value of β the fluid will behave like a Newtonian fluid.

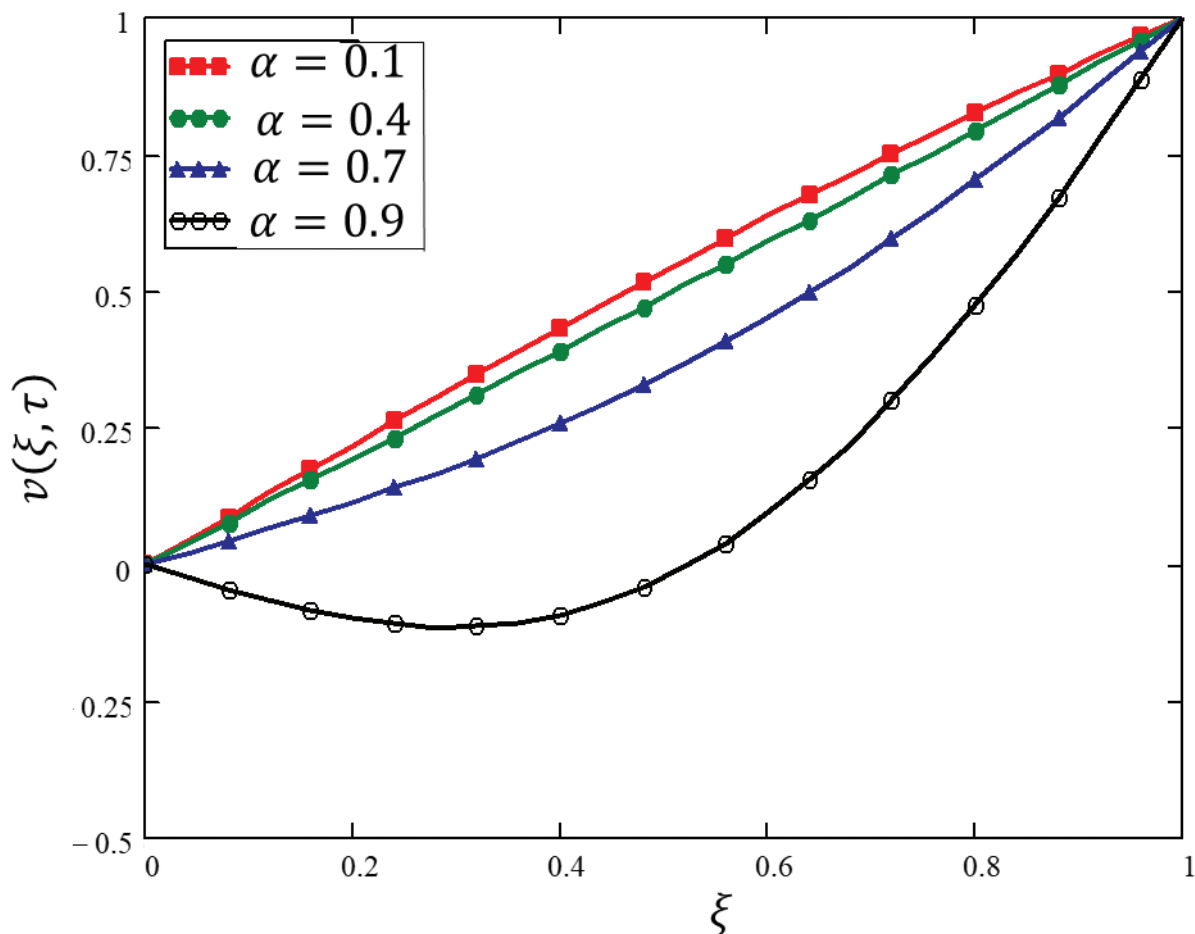


Figure 3: Variations in velocity profile against ξ for different values of α

Table 2: Variations in velocity profile against ξ for different values of α

ξ	$v(\xi, \tau)$ at $\alpha = 0.1$	$v(\xi, \tau)$ at $\alpha = 0.4$	$v(\xi, \tau)$ at $\alpha = 0.7$	$v(\xi, \tau)$ at $\alpha = 0.9$
0	0	0	0	0
0.04	0.044	0.039	0.022	-0.023
0.08	0.088	0.078	0.044	-0.046
0.12	0.131	0.116	0.067	-0.066
0.16	0.175	0.155	0.09	-0.084
0.2	0.219	0.194	0.114	-0.098
0.24	0.262	0.233	0.14	-0.108
0.28	0.305	0.273	0.167	-0.113
0.32	0.348	0.312	0.195	-0.112
0.36	0.39	0.351	0.226	-0.105
0.4	0.433	0.391	0.258	-0.091
0.44	0.474	0.431	0.292	-0.07
0.48	0.516	0.47	0.329	-0.041
0.52	0.557	0.511	0.368	$-3.988e^{-3}$

Table 2 (continued).

ξ	$v(\xi, \tau)$ at $\alpha = 0.1$	$v(\xi, \tau)$ at $\alpha = 0.4$	$v(\xi, \tau)$ at $\alpha = 0.7$	$v(\xi, \tau)$ at $\alpha = 0.9$
0.56	0.597	0.551	0.409	0.041
0.6	0.637	0.591	0.452	0.094
0.64	0.676	0.632	0.498	0.155
0.68	0.715	0.672	0.546	0.224
0.72	0.753	0.713	0.597	0.301
0.76	0.791	0.754	0.649	0.384
0.8	0.828	0.795	0.704	0.474
0.84	0.864	0.836	0.76	0.571
0.88	0.899	0.877	0.818	0.672
0.92	0.934	0.918	0.878	0.778
0.96	0.967	0.959	0.938	0.888
1	1	1	1	1

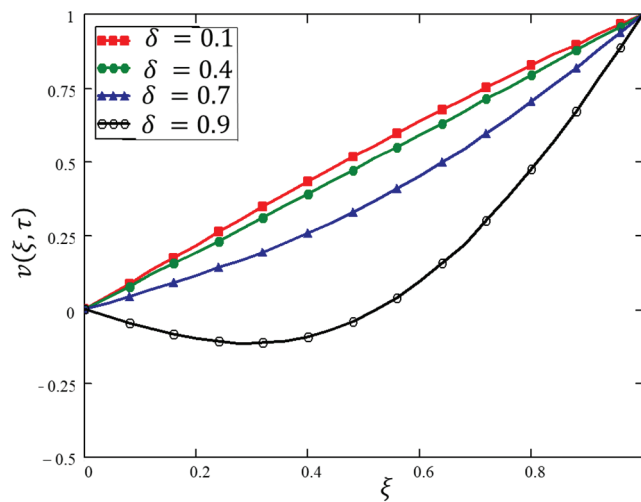


Figure 4: Variations in velocity profile against ξ for different values of δ

Table 3: Variations in velocity profile against ξ for different values of δ

ξ	$v(\xi, \tau)$ at $\delta = 0.1$	$v(\xi, \tau)$ at $\delta = 0.4$	$v(\xi, \tau)$ at $\delta = 0.7$	$v(\xi, \tau)$ at $\delta = 0.9$
0	0	0	0	0
0.04	0.044	0.039	0.022	-0.023
0.08	0.088	0.078	0.044	-0.046
0.12	0.131	0.116	0.067	-0.066
0.16	0.175	0.155	0.09	-0.084
0.2	0.219	0.194	0.114	-0.098
0.24	0.262	0.233	0.14	-0.108
0.28	0.305	0.273	0.167	-0.113
0.32	0.348	0.312	0.195	-0.112

(Continued)

Table 3 (continued).

ξ	$v(\xi, \tau)$ at $\delta = 0.1$	$v(\xi, \tau)$ at $\delta = 0.4$	$v(\xi, \tau)$ at $\delta = 0.7$	$v(\xi, \tau)$ at $\delta = 0.9$
0.36	0.39	0.351	0.226	-0.105
0.4	0.433	0.391	0.258	-0.091
0.44	0.474	0.431	0.292	-0.07
0.48	0.516	0.47	0.329	-0.041
0.52	0.557	0.511	0.368	$-3.988e^{-3}$
0.56	0.597	0.551	0.409	0.041
0.6	0.637	0.591	0.452	0.094
0.64	0.676	0.632	0.498	0.155
0.68	0.715	0.672	0.546	0.224
0.72	0.753	0.713	0.597	0.301
0.76	0.791	0.754	0.649	0.384
0.8	0.828	0.795	0.704	0.474
0.84	0.864	0.836	0.76	0.571
0.88	0.899	0.877	0.818	0.672
0.92	0.934	0.918	0.878	0.778
0.96	0.967	0.959	0.938	0.888
1	1	1	1	1

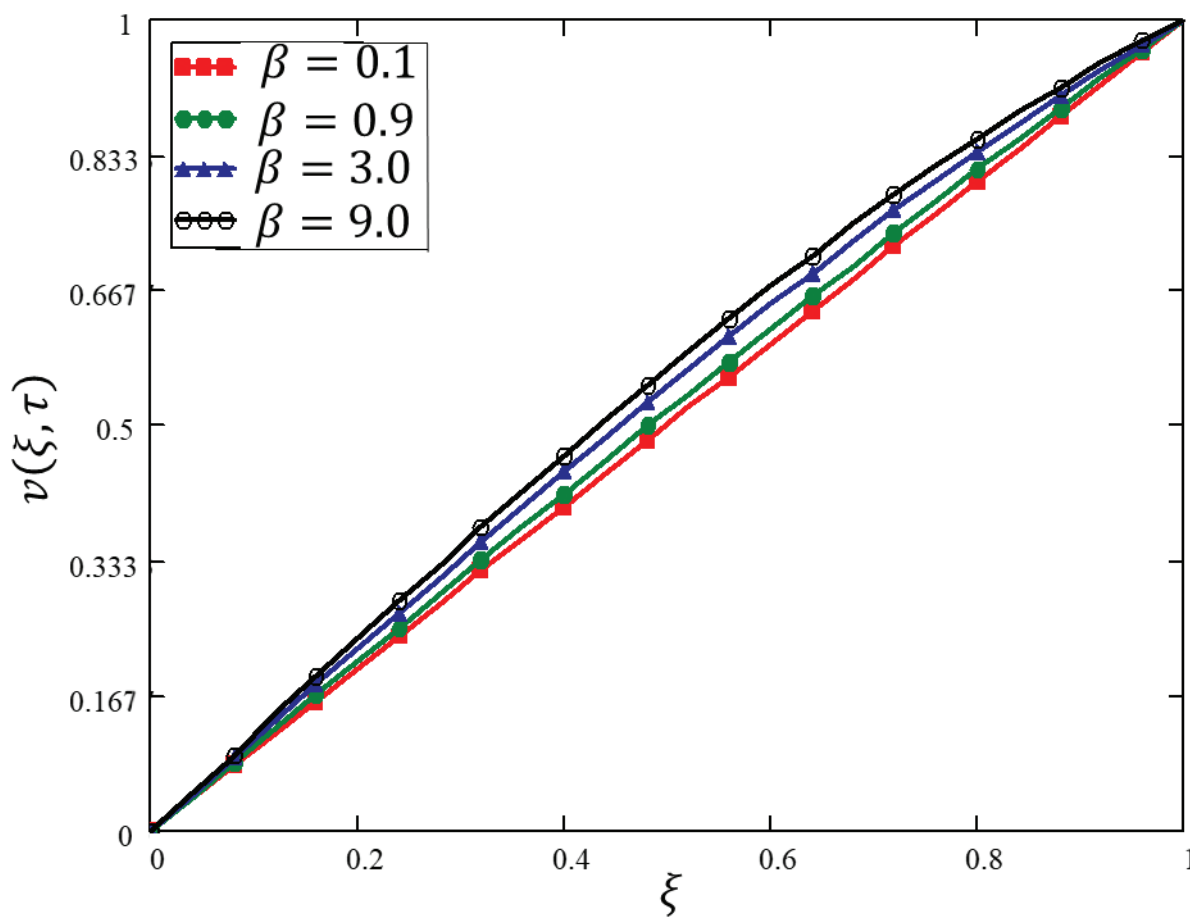


Figure 5: Variations in velocity profile against ξ for different values of β

Table 4: Variations in velocity profile against ξ for different values of β

ξ	$v(\xi, \tau)$ at $\beta = 0.1$	$v(\xi, \tau)$ at $\beta = 0.9$	$v(\xi, \tau)$ at $\beta = 3.0$	$v(\xi, \tau)$ at $\beta = 9.0$
0	0	0	0	0
0.04	0.04	0.042	0.045	0.048
0.08	0.08	0.084	0.09	0.095
0.12	0.12	0.126	0.135	0.142
0.16	0.16	0.168	0.18	0.19
0.2	0.2	0.21	0.225	0.236
0.24	0.24	0.251	0.269	0.283
0.28	0.28	0.293	0.313	0.329
0.32	0.321	0.334	0.357	0.374
0.36	0.361	0.376	0.4	0.419
0.4	0.401	0.417	0.443	0.463
0.44	0.441	0.458	0.486	0.507
0.48	0.481	0.498	0.528	0.55
0.52	0.521	0.539	0.569	0.591
0.56	0.561	0.579	0.609	0.632
0.6	0.601	0.619	0.649	0.672
0.64	0.641	0.659	0.688	0.711
0.68	0.681	0.698	0.727	0.748
0.72	0.721	0.737	0.764	0.785
0.76	0.761	0.776	0.801	0.82
0.8	0.801	0.814	0.837	0.854
0.84	0.84	0.852	0.872	0.886
0.88	0.88	0.89	0.905	0.917
0.92	0.92	0.927	0.938	0.946
0.96	0.96	0.964	0.97	0.974
1	1	1	1	1

4 Conclusion

In this study, a new approach has been used to develop the fractal-fractional model of the Casson fluid. The Laplace transformation technique has been used to solve the model for the exact solutions. The obtained solutions are plotted and presented in tables. The main outcomes of the present study are:

1. The Laplace transform is a better tool to handle the fractal-fractional models.
2. The Casson fluid velocity is higher for the greater values of β , which shows that the fluid will behave like a Newtonian viscous fluid.
3. The variations for different values of α and δ in velocity have been plotted. It is important here to mention that we have separate lines for one value of time. This effect shows the memory effect in the fluid, which cannot be demonstrated from the integer-order model.

Funding Statement: This work was funded by Yayasan Universiti Teknologi PETRONAS (Y.U.T.P.), Cost Center 015LC0-278.

Conflicts of Interest: The authors declare that they have no conflicts of interest to report regarding the present study.

References

- [1] R. Chhabra and J. Richardson, "Flow in pipes and in conduits for non-circular cross-sections," in *Non-Newtonian Flow and Applied Rheology: Engineering Applications*, 2. nd ed., vol. 1. Burlington, USA: Elsevier, pp.110–204, 2008.
- [2] F. Ali, N. A. Sheikh, M. Saqib and I. Khan, "Unsteady MHD flow of second-grade fluid over an oscillating vertical plate with isothermal temperature in a porous medium with heat and mass transfer by using the Laplace transform technique," *Journal of Porous Media*, vol. 20, no. 8, pp. 671–690, 2017.
- [3] T. Sochi, "Flow of non-newtonian fluids in porous media," *Journal of Polymer Science Part B: Polymer Physics*, vol. 48, no. 23, pp. 2437–2767, 2010.
- [4] S. De, J. A. M. Kuipers, E. A. J. F. Peters and J. T. Padding, "Viscoelastic flow simulations in random porous media," *Journal of Non-Newtonian Fluid Mechanics*, vol. 248, pp. 50–61, 2017.
- [5] F. Ali, N. A. Sheikh, M. Saqib and A. Khan, "Hidden phenomena of an MHD unsteady flow in porous medium with heat transfer," *Nonlinear Science Letters A*, vol. 8, no. 1, pp. 101–116, 2017.
- [6] B. Raftari, S. T. Mohyud-Din and A. Yildirim, "Solution to the MHD flow over a non-linear stretching sheet by homotopy perturbation method," *Science China Physics, Mechanics and Astronomy*, vol. 54, no. 2, pp. 342–345, 2011.
- [7] F. Ali, N. A. Sheikh, I. Khan and M. Saqib, "Influence of a porous medium on the hydromagnetic free convection flow of micropolar fluid with radiative heat flux," *Journal of Porous Media*, vol. 21, no. 2, pp. 123–144, 2018.
- [8] M. V. Krishna and G. S. Reddy, "MHD forced convective flow of non-Newtonian fluid through stumpy permeable porous medium," *Materials Today: Proceedings*, vol. 5, no. 1, pp. 175–183, 2018.
- [9] I. Khan, N. A. Shah and D. Vieru, "Unsteady flow of generalized Casson fluid with fractional derivative due to an infinite plate," *European Physical Journal Plus*, vol. 131, no. 6, pp. 181, 2016.
- [10] I. Ullah, S. Shafie and I. Khan, "Effects of slip condition and Newtonian heating on MHD flow of Casson fluid over a nonlinearly stretching sheet saturated in a porous medium," *Journal of King Saud University-Science*, vol. 29, no. 2, pp. 250–259, 2017.
- [11] I. Khan, M. Saqib and F. Ali, "Application of the modern trend of fractional differentiation to the MHD flow of a generalized Casson fluid in a microchannel: Modelling and solution," *European Physical Journal Plus*, vol. 133, no. 7, pp. 262, 2018.
- [12] A. Atangana and R. T. Alqahtani, "Numerical approximation of the space-time Caputo-Fabrizio fractional derivative and application to groundwater pollution equation," *Advances in Difference Equations*, vol. 2016, no. 1, pp. 1–13, 2016.
- [13] N. A. Shah and I. Khan, "Heat transfer analysis in a second grade fluid over and oscillating vertical plate using fractional Caputo–Fabrizio derivatives," *European Physical Journal C*, vol. 76, no. 7, pp. 362, 2016.
- [14] N. A. Sheikh, F. Ali, M. Saqib, I. Khan, S. A. A. Jan *et al.*, "Comparison and analysis of the Atangana–Baleanu and Caputo–Fabrizio fractional derivatives for generalized Casson fluid model with heat generation and chemical reaction," *Results in Physics*, vol. 7, pp. 789–800, 2017.
- [15] F. Ali, N. A. Sheikh, I. Khan and M. Saqib, "Magnetic field effect on blood flow of Casson fluid in axisymmetric cylindrical tube: A fractional model," *Journal of Magnetism Magnetic Materials*, vol. 423, pp. 327–336, 2017.
- [16] F. Ali, N. A. Sheikh, I. Khan and M. Saqib, "Solutions with Wright function for time fractional free convection flow of Casson fluid," *Arabian Journal for Science Engineering*, vol. 42, no. 6, pp. 2565–2572, 2017.
- [17] N. A. Sheikh, F. Ali, M. Saqib, I. Khan and S. A. A. Jan, "A comparative study of Atangana–Baleanu and Caputo–Fabrizio fractional derivatives to the convective flow of a generalized Casson fluid," *European Physical Journal Plus*, vol. 132, no. 1, pp. 54, 2017.
- [18] M. Saqib, F. Ali, I. Khan, N. A. Sheikh, S. A. A. Jan *et al.*, "Exact solutions for free convection flow of generalized Jeffrey fluid: A Caputo-Fabrizio fractional model," *Alexandria Engineering Journal*, vol. 57, no. 3, pp. 1849–1858, 2018.
- [19] M. Saqib, I. Khan and S. Shafie, "Application of Atangana–Baleanu fractional derivative to MHD channel flow of CMC-based-CNT's nanofluid through a porous medium," *Chaos, Solitons & Fractals*, vol. 116, pp. 79–85, 2018.

- [20] N. A. Sheikh, D. L. C. Ching, I. Khan, D. Kumar and K. S. Nisar, "A new model of fractional Casson fluid based on generalized Fick's and Fourier's laws together with heat and mass transfer," *Alexandria Engineering Journal*, vol. 59, no. 5, pp. 2865–2876, 2019.
- [21] A. Carpinteri and F. Mainardi, "Fractional calculus: Some basic problems in continuum and statistical mechanics," in *Fractals and Fractional Calculus in Continuum Mechanics*, 1. st ed., vol. 1. New York, USA: Springer, pp.291–347, 2014.
- [22] K. A. Abro and A. Atangana, "A comparative study of convective fluid motion in rotating cavity via Atangana–Baleanu and Caputo–Fabrizio fractal-fractional differentiations," *European Physical Journal Plus*, vol. 135, no. 2, pp. 226, 2020.
- [23] M. A. Imran, "Application of fractal fractional derivative of power law kernel (FFPD α,β) to MHD viscous fluid flow between two plates," *Chaos, Solitons & Fractals*, vol. 134, pp. 109691, 2020.
- [24] W. Wei, J. Yongbin, L. Yanhong, L. Ji, W. Xin *et al.*, "An advanced deep residual dense network (DRDN) approach for image super-resolution," *International Journal of Computational Intelligence Systems*, vol. 12, no. 2, pp. 1592–1601, 2019.
- [25] Z. Zhang, Y. Li, C. Wang, M. Wang, Y. Tu *et al.*, "An ensemble learning method for wireless multimedia device identification," *Security and Communication Networks*, vol. 2018, pp. 1–9, 2018.
- [26] L. He, J. Wang, H. Bai, Y. Jiang and T. Li, "A novel parallel and distributed magnetotelluric inversion algorithm on multi-threads workloads cluster," *Cluster Computing*, vol. 22, no. 4, pp. 1073–1083, 2019.
- [27] Y. Jiang, M. Zhao, C. Hu, L. He, H. Bai *et al.*, "A parallel FP-growth algorithm on World Ocean Atlas data with multi-core CPU," *Journal of Supercomputing*, vol. 75, no. 2, pp. 732–745, 2019.
- [28] Z. Min, G. Yang, J. Wang and G. J Kim, "A privacy-preserving BGN-type parallel homomorphic encryption algorithm based on LWE," *Journal of Internet Technology*, vol. 20, no. 7, pp. 2189–2200, 2019.
- [29] N. A. Sheikh, F. Ali, I. Khan and M. Saqib, "A modern approach of Caputo–Fabrizio time-fractional derivative to MHD free convection flow of generalized second-grade fluid in a porous medium," *Neural Computing and Applications*, vol. 30, no. 6, pp. 1865–1875, 2018.
- [30] M. Goodarzi, M. R. Safaei, K. Vafai, G. Ahmadi, M. Dahari *et al.*, "Investigation of nanofluid mixed convection in a shallow cavity using a two-phase mixture model," *International Journal of Thermal Sciences*, vol. 75, pp. 204–220, 2014.
- [31] B. Xiong, K. Yang, J. Zhao, W. Li and K. Li, "Performance evaluation of OpenFlow-based software-defined networks based on queueing model," *Computer Networks*, vol. 102, pp. 172–185, 2016.
- [32] X. Su, X. Liu, J. Lin, S. He, Z. Fu *et al.*, "De-cloaking malicious activities in smartphones using HTTP flow mining," *TIIIS*, vol. 11, no. 6, pp. 3230–3253, 2017.
- [33] M. Lin, Q. Feng, J. Chen and W. Li, "Partition on trees with supply and demand: Kernelization and algorithms," *Theoretical Computer Science*, vol. 657, pp. 11–19, 2017.
- [34] F. Peng, D. I Zhou, M. Long and X. M Sun, "Discrimination of natural images and computer generated graphics based on multi-fractal and regression analysis," *AEU: International Journal of Electronics and Communications*, vol. 71, pp. 72–81, 2017.
- [35] T. Abdeljawad, "Fractional operators with generalized Mittag-Leffler kernels and their differintegrals," *Chaos*, vol. 29, no. 2, pp. 023102, 2019.
- [36] J. F. Gomez-Aguilar, T. Cordova-Fraga, T. Abdeljawad, A. Khan and H. Khan, "Analysis of fractal-fractional malaria transmission model," *Fractals*, vol. 12, no. 4, pp. 2040041, 2020.
- [37] B. Acay, T. Abdeljawad and E. Bas, "Fractional economic models based on market equilibrium in the frame of different type kernels," *Chaos, Solitons and Fractals*, vol. 130, pp. 109438, 2020.
- [38] K. Shah, T. Abdeljawad, I. Mahariq and F. Jarad, "Qualitative analysis of a mathematical model in the time of COVID-19," *BioMed Research International*, vol. 2020, pp. 1–11.
- [39] R. U. Din, K. Shah, I. Ahmad and T. Abdeljawad, "Study of transmission dynamics of novel COVID-19 by using mathematical model," *Advances in Difference Equations*, vol. 323, 2020. (In press). Available: <https://www.preprints.org/manuscript/202005.0164/v1>

- [40] S. Aman, I. Khan, Z. Ismail, M. Z. Salleh, A. S. Alshomrani *et al.*, “Magnetic field effect on Poiseuille flow and heat transfer of carbon nanotubes along a vertical channel filled with Casson fluid,” *AIP Advances*, vol. 7, no. 1, pp. 1–18, 2017.
- [41] L. A. Lund, Z. Omar, J. Raza, I. Khan and E. S. M. Sherif, “Effects of Stefan blowing and slip conditions on unsteady MHD Casson nanofluid flow over an unsteady shrinking sheet: Dual solutions,” *Symmetry*, vol. 12, no. 3, pp. 487, 2020.
- [42] F. Ali, N. Khan, A. Imtiaz, I. Khan and N. A. Sheikh, “The impact of magnetohydrodynamics and heat transfer on the unsteady flow of Casson fluid in an oscillating cylinder via integral transform: A Caputo–Fabrizio fractional model,” *Pramana*, vol. 93, no. 3, pp. 47, 2019.
- [43] A. Atangana, “Fractal-fractional differentiation and integration: Connecting fractal calculus and fractional calculus to predict complex system,” *Chaos, Solitons & Fractals*, vol. 102, pp. 396–406, 2017.